Minor Groove-Directed and Intercalative Ligand−DNA Interactions in the Poisoning of Human DNA Topoisomerase I by Protoberberine Analogs[†]

Daniel S. Pilch,*[,‡] Chiang Yu,[‡] Darshan Makhey,[§] Edmond J. LaVoie,[§] A. R. Srinivasan,[||] Wilma K. Olson,[||] Ronald R. Sauers,[||] Kenneth J. Breslauer,[||] Nicholas E. Geacintov,[⊥] and Leroy F. Liu[‡]

Department of Pharmacology, University of Medicine and Dentistry of New Jersey, Robert Wood Johnson Medical School, Piscataway, New Jersey 08854, Departments of Pharmaceutical Chemistry and Chemistry, Rutgers−The State University of New Jersey, Piscataway, New Jersey 08855, and Department of Chemistry, New York University, New York, New York 10003

Received May 29, 1997; Revised Manuscript Received July 28, 1997[⊗]

ABSTRACT: Spectroscopic, calorimetric, DNA cleavage, electrophoretic, and computer modeling techniques have been employed to characterize the DNA binding and topoisomerase poisoning properties of three protoberberine analogs, 8-desmethylcoralyne (DMC), 5,6-dihydro-8-desmethylcoralyne (DHDMC), and palmatine, which differ in the chemical structures of their B- and/or D-rings. DNA topoisomerase-mediated cleavage assays revealed that these compounds were unable to poison mammalian type II topoisomerase. By contrast, the three protoberberine analogs poisoned human topoisomerase I according to the following hierarchy: DHDMC > DMC > palmatine. DNA binding by all three protoberberine analogs induced negative flow linear dichroism signals as well as unwinding of the host duplex. These two observations are consistent with an intercalative mode of protoberberine binding to duplex DNA. However, a comparison of the DNA binding properties for DMC and DHDMC, which differ only by the state of saturation at the 5,6 positions of the B-ring, revealed that the protoberberine analogs do not "behave" like classic DNA intercalators. Specifically, saturation of the 5−6 double bond in the B-ring of DMC, thereby converting it to the DHDMC molecule, was associated with enhanced DNA unwinding as well as a reversal of DNA binding preference from a DNA duplex with an inaccessible or occluded minor groove {poly[d(G-C)]$_2$} to DNA duplexes with accessible or unobstructed minor grooves {poly[d(A-T)]$_2$ and poly[d(I-C)]$_2$}. In addition, a comparison of the DNA binding properties for DHDMC and palmatine revealed that transferring the 11-methoxy moiety on the D-ring of DHDMC to the 9 position, thereby converting it to palmatine, was associated with a reduction in binding affinity for both duplexes with unobstructed minor grooves as well as for duplexes with occluded minor grooves. These DNA binding properties are consistent with a "mixed-mode" DNA binding model for protoberberines in which a portion of the ligand molecule intercalates into the double helix, while the nonintercalated portion of the ligand molecule protrudes into the minor groove of the host duplex, where it is thereby available for interactions with atoms lining the floor and/or walls of the minor groove. Furthermore, saturation at the 5,6 positions of the B-ring, which causes the A-ring to be tilted relative to the plane formed by rings C and D, appears to stabilize the interaction between the host duplex and the minor groove-directed portion of the protoberberine ligand. Computer modeling studies on the DHDMC−poly[d(A-T)]$_2$ complex suggest that this interaction may involve van der Waals contacts between the ligand A-ring and backbone sugar atoms lining the minor groove of the host duplex. The hierarchy of topoisomerase I poisoning noted above suggests that this minor groove-directed interaction may play an important role in topoisomerase I poisoning by protoberberine analogs. In the aggregate, our results presented here, coupled with the recent demonstration of topoisomerase I poisoning by minor groove-binding terbenzimidazoles [Sun, Q., Gatto, B., Yu, C., Liu, A., Liu, L. F., & LaVoie, E. J. (1995) *J. Med. Chem. 38*, 3638−3644], suggest that minor groove-directed ligand−DNA interactions may be of general importance in the poisoning of topoisomerase I.

Topoisomerase I has been established as an attractive molecular target for anticancer drugs, primarily due to the successful development of the camptothecin family of compounds into the clinic (Potmesil & Pinedo, 1995). Camptothecin has been shown to inhibit the religation step of the topoisomerase I reaction, thereby resulting in the accumulation of an enzyme−DNA−drug, ternary cleavable complex (Hsiang et al., 1985, 1989; Porter & Champoux, 1989). In addition to the camptothecins, numerous new compounds, including nitidine (Wang et al., 1993), fagaronine (Wang et al., 1993), bulgarein (Fujii et al., 1993), intoplicine (RP-60475) (Poddevin et al., 1993), saintopin (Yamashita et al., 1991; Leteurtre et al., 1994), the indolocarbazoles (Yamashita et al., 1992; Yoshinari et al., 1993; Kanzawa et al., 1995), the protoberberines (Makhey et al., 1995, 1996; Gatto et al., 1996), and the mono- (Kim et al., 1996b), bi- (Chen et al., 1993a,b; Sun et al., 1994; Kim et al., 1996a), and terbenzimidazoles (Sun et al., 1995), recently

[†] This work was supported by National Institutes of Health Grants GM23509 (K.J.B.), GM34469 (K.J.B.), CA47995 (K.J.B.), GM20861 (W.K.O.), and CA39962 (L.F.L.).

* To whom correspondence should be addressed: Tel., 732-445-3954; Fax, 732-445-5312; e-mail, pilch@rutchem.rutgers.edu.

[‡] UMDNJ−Robert Wood Johnson Medical School.

[§] Department of Pharmaceutical Chemistry, Rutgers University.

[||] Department of Chemistry, Rutgers University.

[⊥] New York University.

[⊗] Abstract published in *Advance ACS Abstracts,* October 1, 1997.

S0006-2960(97)01272-5 CCC: $14.00

have been identified as poisons of mammalian DNA topoisomerase I.

Recent studies, in which alkylating camptothecin derivatives were employed, have suggested that camptothecin binds to the enzyme−DNA interface (Hertzberg et al., 1990; Pommier et al., 1995). Equilibrium dialysis studies revealed an absence of DNA binding by camptothecin in a Tris-HCl buffer (pH 7.4) containing 50 mM NaCl (Hsiang et al., 1985). However, all the newly identified topoisomerase I poisons, with the exception of the monobenzimidazoles (D. S. Pilch, unpublished results), are known to bind to duplex DNA (Zee-Cheng & Cheng, 1973; Wilson et al., 1976; Davidson et al., 1977; Pjura et al., 1987; Debnath et al., 1991; Yamashita et al., 1991, 1992; Chen et al., 1993b; Fujii et al., 1993; Poddevin et al., 1993; Wang et al., 1993; Yoshinari et al., 1993; Spink et al., 1994; Saran et al., 1995; Clark et al., 1996; Pilch et al., 1996). In addition, many compounds recently identified as poisons of topoisomerase I exhibit topoisomerase II poisoning activity as well. These dual topoisomerase poisons include actinomycin D (Trask & Muller, 1988; Wassermann et al., 1990), morpholinyldoxorubicin (Wassermann et al., 1990), saintopin (Yamashita et al., 1991; Leteurtre et al., 1994), intoplicine (Poddevin et al., 1993), nitidine (Wang et al., 1993; Makhey et al., 1995, 1996), and the protoberberines (Makhey et al., 1995, 1996). In the aggregate, these findings suggest that DNA binding may be important for the poisoning of both the type I and type II topoisomerases. For drugs that target topoisomerase II, drug intercalation into the host DNA duplex is strongly correlated with enzyme poisoning (Bodley et al., 1989). However, the mechanism of action of drugs that target topoisomerase I is much less clear. Although some of the new topoisomerase I poisons, such as actinomycin D (Müller & Crothers, 1968; Sobell & Jain, 1972; Takusagawa et al., 1982), morpholinyldoxorubicin (Wassermann et al., 1990), the protoberberines (Wilson et al., 1976; Davidson et al., 1977; Saran et al., 1995), and the indolocarbazoles (Yamashita et al., 1992; Yoshinari et al., 1993), exhibit properties characteristic of intercalation into the host duplex, the strength of intercalation, at least in the case of the indolocarbazoles (Yamashita et al., 1992), does not appear to be correlated with topoisomerase I poisoning. Portions of both the actinomycin D and morpholinyldoxorubicin molecules are known to interact with the minor groove of the host duplex (Sobell & Jain, 1972; Takusagawa et al., 1982; Wassermann et al., 1990). Hence, these drugs exhibit both intercalative and minor groove-directed interactions with the host DNA duplex ("mixed-mode" DNA binding).

To date, no firm correlation has been established between the minor groove-directed interactions exhibited by mixed-mode DNA binders (e.g., actinomycin D and morpholinyldoxorubicin) and their topoisomerase I poisoning activities. However, several recent studies have suggested that DNA minor groove binding may be involved in topoisomerase I poisoning. Specifically, a number of ligands (including the bibenzimidazoles, Hoechst 33342 and 33258, and various terbenzimidazole derivatives) whose primary mode of DNA binding is through an interaction with the DNA minor groove (Pjura et al., 1987; Parkinson et al., 1990; Fede et al., 1991, 1993; Spink et al., 1994; Pilch et al., 1996) have been identified as specific poisons of topoisomerase I (Chen et al., 1993a, 1993b; Sun et al., 1994, 1995; Kim et al., 1996a). In addition, binding by the new topoisomerase I poison, bulgarein, was shown to induce winding rather than unwinding of the host DNA duplex (Fujii et al., 1993). This observation may be indicative of an interaction between bulgarein and the minor groove of the host duplex, since the binding of netropsin, a known DNA minor groove binder, also induces winding of the host DNA duplex (Pilch et al., 1995). While the findings noted above have suggested a possible role for DNA minor groove binding in topoisomerase I poisoning, this potential role has been blurred somewhat due to the demonstration that Hoechst 33342 also can unwind the host DNA duplex (Chen et al., 1993a). To broaden our base of knowledge of the role ligand−DNA interactions play in topoisomerase I poisoning, we have begun a program in which we are characterizing the topoisomerase I poisoning and DNA binding properties of various families of structurally related nucleic acid-binding ligands.

In this work, we characterize the topoisomerase I poisoning and DNA binding properties of three protoberberine analogs, 8-desmethylcoralyne (DMC),[1] 5,6-dihydro-8-desmethylcoralyne (DHDMC), and palmatine, which differ in the chemical structures of their B- and/or D-rings. Our results reveal that the three protoberberine analogs poison human topoisomerase I according to the hierarchy DHDMC > DMC > palmatine but do not poison mammalian topoisomerase II. DNA binding studies indicate that the protoberberines weakly unwind duplex DNA but also are capable of distinguishing between duplexes with accessible (unobstructed) and inaccessible (occluded) minor grooves. These DNA binding properties are consistent with a mixed mode of DNA binding, in which a portion of the ligand molecule intercalates into the double helix and the nonintercalated portion protrudes into and interacts with the minor groove of the host duplex. A comparison of the DNA binding and topoisomerase I poisoning data reveals that saturation at the 5,6 positions of the B-ring is accompanied by enhanced binding to duplexes with open or accessible minor grooves as well as enhanced topoisomerase I poisoning. This observation suggests that a DNA minor groove-directed interaction is important in topoisomerase I poisoning by protoberberines. In conjunction with the recent demonstration of topoisomerase I-specific poisoning by minor groove binding bi- and terbenzimidazoles (Chen et al., 1993a,b; Sun et al., 1994, 1995; Kim et al., 1996a), our results presented here suggest the possibility of a general correlation between minor groove-directed ligand−DNA interactions and the poisoning of topoisomerase I.

MATERIALS AND METHODS

Enzyme, DNA, and Ligand Molecules. Recombinant human DNA topoisomerase I (hTOP1) was isolated from *Escherichia coli* BL21(DE3) as described previously (Gatto et al., 1996). The camptothecin-resistant hTOP1, CPT-K5 TOP1, was isolated by a similar procedure (Gatto et al., 1996). Synthetic DNA polymers and salmon testes DNA were obtained from Pharmacia Biotech, Inc. (Piscataway, NJ), and were used without further purification. Concentra-

[1] Abbreviations: poly[d(A-T)]$_2$, duplex of alternating poly(dA-dT); poly[d(I-C)]$_2$, duplex of alternating poly(dI-dC); poly[d(G-C)]$_2$, duplex of alternating poly(dG-dC); TOP, topoisomerase; DMC, 8-desmethylcoralyne; DHDMC, 5,6-dihydro-8-desmethylcoralyne; CPT, camptothecin; EtBr, ethidium bromide; VM-26, teniposide; EDTA, disodium salt of ethylenediaminetetraacetic acid; bp, base pair(s); r_{bp}, [total ligand]/[base pairs]; WC, Watson−Crick; T_m, melting temperature; LD, linear dichroism; DSC, differential scanning calorimetry; UV−vis, ultraviolet−visible.

tions of all nucleic acid polymers were determined spectrophotometrically using the following extinction coefficients in units of (mol of base/L)$^{-1}$ cm^{-1}: $\epsilon_{262} = 6600$ for poly(dA-dT)·poly(dA-dT) {≡poly[d(A-T)]$_2$}, $\epsilon_{251} = 6900$ for poly(dI-dC)·poly(dI-dC) {≡poly[d(I-C)]$_2$}, and $\epsilon_{254} = 8400$ for poly(dG-dC)·poly(dG-dC) {≡poly[d(G-C)]$_2$}. The concentrations of all salmon testes DNA solutions also were determined spectrophotometrically by assuming that one A_{260} unit/mL of salmon testes DNA corresponds to a concentration of 50 μg/mL. Palmatine was obtained from Aldrich Chemical Co. (Milwaukee, WI), while ethidium bromide (EtBr) was obtained from Sigma Chemical Co. (St. Louis, MO). Both drugs were used without further purification. Camptothecin (CPT) was obtained from the Drug Synthesis and Chemistry Branch of the Division of Cancer Treatment at the National Cancer Institute (Bethesda, MD), while teniposide (VM-26) was a generous gift from Bristol-Myers Squibb (Lawrenceville, NJ). 8-Desmethylcoralyne (DMC) and 5,6-dihydro-8-desmethylcoralyne (DHDMC) were synthesized as described previously (Makhey et al., 1995, 1996).

Topoisomerase Cleavage Assays. Topoisomerase cleavage assays were conducted as previously reported (Hsiang et al., 1985; Bodley et al., 1989; Chen et al., 1993a). The plasmid, YEpG, was linearized with *Bam*HI and 3′-end-labeled as previously described (Chen et al., 1993a).

DNA Unwinding Assay. The DNA unwinding assay used to measure the relative strength of DNA intercalation was conducted in essentially the same manner as described previously (Bodley et al., 1989) using a mixture of supercoiled and relaxed YEpG DNA as substrates, with the exception that the camptothecin-resistant hTOP1, CPT-K5, was used in place of the wild-type enzyme. Electrophoresis was performed at room temperature in buffer containing 80 mM Tris−phosphate (pH 8.3) and 2 mM EDTA (TPE buffer). Inhibition of TOP1 catalytic activity by the DNA binding ligands, if present, is revealed by the presence of two groups of bands rather than a single Gaussian distribution of the topoisomers. The total degree of unwinding can be determined by comparing the Gaussian centers of the topoisomers.

UV−vis Spectrophotometry. All UV−vis absorbance experiments were conducted on an AVIV Model 14DS spectrophotometer (Aviv Associates; Lakewood, NJ) equipped with a thermoelectrically controlled cell holder. A quartz cell with a 1 cm path length was used for all the absorbance studies. Isothermal (25 °C) absorption spectra for the linear dichroism experiments were acquired from 220 to 500 nm. The salmon testes DNA solutions were 50 μM in base pair and contained 10 mM sodium phosphate (pH 6.8), 0.1 mM EDTA, and either 10 μM DMC or 10 μM DHDMC.

Absorbance versus temperature profiles were measured at either 242 or 260 nm in PE buffer [2 mM sodium phosphate (pH 7.0), 0.1 mM EDTA] with a 6 s averaging time. The temperature was raised in 0.3 °C increments, and the samples were allowed to equilibrate for 1 min at each temperature setting. For each optically detected transition, the melting temperature (T_m) was determined as previously described (Marky & Breslauer, 1987a). The DNA polymer concentrations were 15 μM in base pair, while the ligand concentrations ranged from 0 to 7.5 μM.

Flow Linear Dichroism Measurements. Flow linear dichroism measurements were conducted as previously described (Geacintov et al., 1987). Each flow linear dichroism spectrum shown in panel B of Figure 4 was acquired from 240 to 440 nm and reflects the average of two scans. A Couette cell with a total optical path length of 1.2 mm was used for all the linear dichroism studies. The salmon testes DNA solutions were 50 μM in base pair and contained 10 mM sodium phosphate (pH 6.8), 0.1 mM EDTA, and either 10 μM DMC or 10 μM DHDMC.

Differential Scanning Calorimetry (DSC). Heat capacity (ΔC_p) versus temperature (T) profiles for the thermally induced transitions of solutions containing either poly[d(A-T)]$_2$, poly[d(I-C)]$_2$, or poly[d(G-C)]$_2$ were measured in PE buffer using a prototype Model 5100 Nano Calorimeter (Calorimetry Science Corp., Provo, UT). In these experiments, the heating rate was 1 °C/min. Transition enthalpies (ΔH_{WC}) were calculated from the areas under the heat capacity curves using the Origin version 4.1 software (MicroCal, Inc., Northampton, MA). The DNA polymer solutions were 200 μM in base pair.

Isothermal, Stopped-Flow Mixing Microcalorimetry. Isothermal calorimetric measurements were performed at 20 °C using an all tantalum, differential, stopped-flow, heat conduction microcalorimeter (model DSFC-100; Commonwealth Technology, Inc., Alexandria, VA), developed by Mudd and Berger (Mudd & Berger, 1988; Remeta et al., 1991). In a typical experiment, the reaction is initiated by a microprocessor-controlled stepping motor that activates a syringe drive which delivers, within 0.6 s, 80 μL of each reagent (100 μM base pair DNA and 50 μM ligand) into tantalum mixing chambers, with distilled water being used in the reference mixing chamber. A delay of 300 s was used between each injection/reaction. Each reaction generated a heat burst curve (μJ/s vs s), with the area under the curve being determined by integration to obtain the heat for that reaction, which ranged from 80 to 97 μJ for the DMC experiments, from 63 to 99 μJ for the DHDMC experiments, and from 48 to 64 μJ for the palmatine experiments. When compared with observed ligand−buffer mixing heats of 67, 23, and 23 μJ for DMC, DHDMC, and palmatine, respectively, these data reflect signal-to-noise ratios ranging from 1.2 to 4.3. No significant integral heats of dilution were observed for any of the DNA polymers. The calorimeter was calibrated chemically by measuring the heat associated with a 1:2 dilution of 10 mM NaCl (Robinson, 1932; Gulbransen & Robinson, 1934).

Computer Modeling of the DHDMC−Poly[d(A-T)]$_2$ Complex. Theoretical modeling of the DHDMC−poly[d(A-T)]$_2$ complex was conducted in two stages. The first stage entailed the identification of low-energy duplex conformations, in which adjacent base pairs were separated sufficiently so as to accommodate insertion of a DHDMC molecule. A constrained molecular modeling method (Srinivasan & Olson, 1987) was used to construct the duplex. The coordinates for Watson−Crick base pairs in a standard B-DNA conformation were used as the starting point of the calculations (Chandrasekaran & Arnott, 1989). Possible polymer building blocks that connect successive bases on each of the two strands then were identified by an exhaustive search of chain backbone conformation space. The base pair rise was set to 6.8 Å and the helical twist angle to 10° in all duplex structures. These values, which correspond to a B-DNA duplex unwinding angle of 26°, fall within the limits of the known geometries of drug−nucleic acid intercalation complexes as derived from X-ray (Berman & Young, 1981), sedimentation velocity (Crawford & Waring, 1967; Bauer

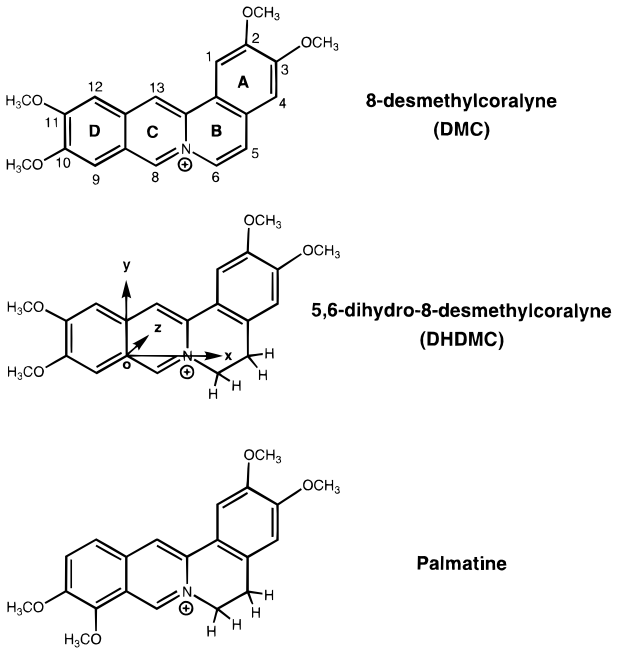

FIGURE 1: Chemical structures of 8-desmethylcoralyne (DMC), 5,6-dihydro-8-desmethylcoralyne (DHDMC), and palmatine. The atomic numbering and ring lettering are indicated in the structure of DMC (top), while the *x*, *y*, *z* coordinate reference frame used in the computer modeling of the DHDMC−poly[d(A-T)]$_2$ complex is indicated in the structure of DHDMC (center).

& Vinograd, 1968), and gel electrophoresis studies (Keller, 1975).

The unbound polymer duplex of lowest computed potential energy then was used in positioning the DHDMC molecule in the second stage of modeling. In the absence of a crystal structure for the DNA-free DHDMC molecule, starting coordinates were taken from the crystal structure of berberine chloride (Kariuki & Jones, 1995), which differs from DHDMC in that it contains (i) a 9,10-dimethoxy instead of a 10,11-dimethoxy substitution on its D-ring and (ii) a 2,3-methylenedioxy instead of a 2,3-dimethoxy substitution on its A-ring. After the berberine molecule was converted to DHDMC by making the appropriate modifications, the coordinates of the modified drug molecule were transformed to a new reference frame in which the *x*−*y* plane coincided with the plane formed by rings C and D of the drug (Figure 1). The drug was initially placed halfway between the reference base pair and its neighbor in the duplex model. Numerous structures were generated by rotating the DHDMC molecule about the *x*-, *y*-, and *z*-axes, as well as by translations along the *x*- and *y*-axes. Rotations about the *z*-axis were varied in 10° intervals from 0° to 350°. Rotations about the *x*- and *y*-axes, which are analogous to the rolling and tilting motions of a standard Watson−Crick base pair in a B-DNA duplex, were varied in 5° intervals from −10° to +10°. The *x* and *y* translations were varied in 1 Å increments from −6 Å to +6 Å. These rotations and translations facilitated the identification of an energetically stable location for the intercalating ligand within the rigid duplex framework. At each ligand position, the potential energy of the ligand−duplex complex was determined using a standard potential energy function in which van der Waals contributions (both repulsive and attractive) were estimated by a 6-12 potential (Zhurkin et al., 1980; Poltev & Shulyupina, 1986).

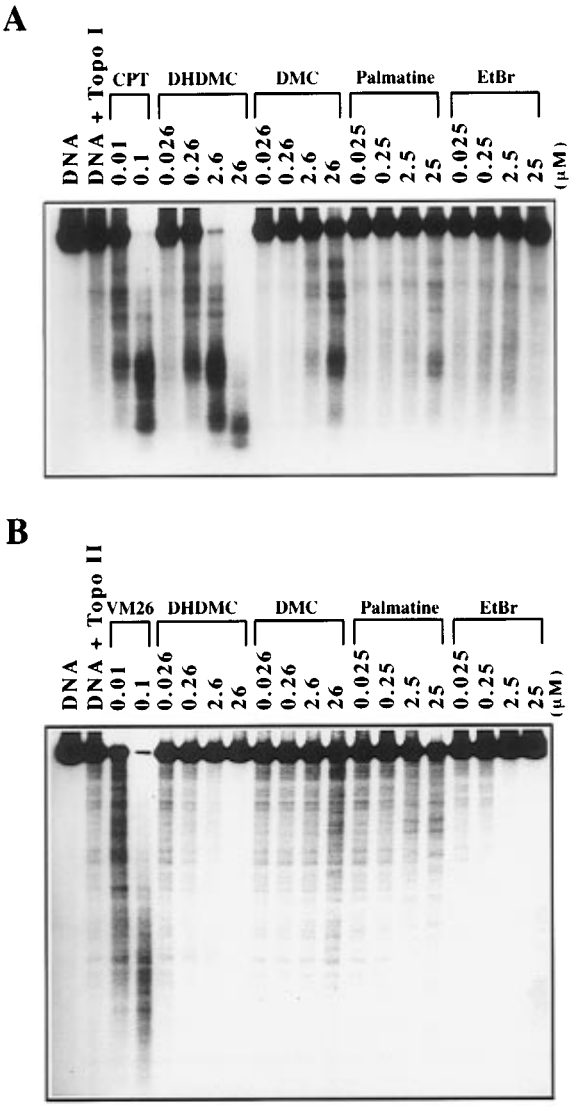

FIGURE 2: Agarose gels showing topoisomerase-mediated DNA cleavage in the presence of the protoberberines, ethidium bromide (EtBr), and either camptothecin (CPT) (panel A) or teniposide (VM-26) (panel B). (A) Agarose gel showing TOP1-mediated DNA cleavage, with the ligands and their concentrations indicated at the tops of the lanes. Following incubation with both TOP1 and ligand, the DNA samples were treated with SDS and proteinase K and then alkali-denatured prior to loading onto a 0.8% agarose gel in TPE buffer. (B) Agarose gel showing TOP2-mediated DNA cleavage, with the ligands and their concentrations indicated at the tops of the lanes. Following incubation with both TOP2 and ligand, the DNA samples were loaded directly onto a 0.8% agarose gel in TPE buffer.

RESULTS

DHDMC Stimulates Human TOP1-Mediated DNA Cleavage to a Greater Extent Than either DMC or Palmatine. We compared the abilities of DHDMC, DMC, and palmatine to poison human TOP1 by measuring the relative extents to which they stimulate TOP1-mediated DNA cleavage. The resulting cleavage patterns are shown in panel A of Figure 2. Inspection of Figure 2A reveals that DHDMC stimulates TOP1-mediated DNA cleavage in a manner dependent on its concentration. By contrast, palmatine does not stimulate TOP1-mediated DNA cleavage above the background level over an identical range of ligand concentrations. Further inspection of Figure 2A reveals that a DMC concentration of 26 μM is required to induce the same approximate level of TOP1-mediated DNA cleavage induced by a DHDMC

concentration of only 0.26 μM. Thus, DHDMC is a roughly 100-fold more potent stimulator of TOP1-mediated DNA cleavage than DMC. In the aggregate, our results indicate that the TOP1 poisoning capacities of the three protoberberine analogs studied here follow the hierarchy DHDMC > DMC > palmatine. As discussed below, this hierarchy of TOP1 poisoning correlates with the strength and mode of DNA binding exhibited by the three ligands.

Neither of the Three Protoberberine Analogs Stimulates TOP2-Mediated DNA Cleavage. We compared the abilities of DHDMC, DMC, and palmatine to poison mammalian TOP2 by measuring the relative extents to which they stimulate calf thymus TOP2-mediated DNA cleavage. The resulting cleavage patterns are shown in panel B of Figure 2. Inspection of Figure 2B reveals that neither of the three protoberberine analogs stimulates TOP2-mediated DNA cleavage above the background level, an observation indicating that these three compounds are not TOP2 poisons. The lack of TOP2 poisoning exhibited by DMC and palmatine echoes their minimal abilities to poison TOP1 (Figure 2A). However, the inability of DHDMC to poison TOP2 contrasts with its potent TOP1 poisoning activity (Figure 2A). This specificity for TOP1 versus TOP2 poisoning by DHDMC may be correlated with its mode of DNA binding, which, as discussed below, exhibits properties characteristic of both intercalation and a minor groove-directed interaction.

Further inspection of Figure 2B reveals that DHDMC not only fails to stimulate TOP2-mediated DNA cleavage above the background level but, at its higher concentrations (26−260 μM), also inhibits the background DNA cleavage. This behavior also is exhibited by the strong DNA intercalator, ethidium bromide (EtBr), but is not exhibited by DMC and palmatine, which, as shown below, exhibit lower overall DNA binding affinities than DHDMC. Hence, the concentration-dependent inhibition of background TOP2-mediated DNA cleavage by DHDMC is likely correlated with its DNA binding strength.

All Three Protoberberine Analogs Unwind Duplex DNA, with the Extent of Unwinding Being Greater for DHDMC Than for either DMC or Palmatine. DNA unwinding measurements were conducted to assess the impact, if any, of DHDMC, DMC, and palmatine on the superhelical state of circular duplex DNA. The resulting unwinding profiles are shown in Figure 3. In these experiments, ligand-induced DNA unwinding is revealed by an upward and subsequent downward shift in the mobilities of the Gaussian centers of the topoisomers as a function of increasing ligand concentration. Inspection of Figure 3 reveals that all three protoberberine analogs unwind duplex DNA in a concentration-dependent manner, an observation consistent with an intercalative mode of protoberberine binding to DNA. However, even at a concentration of 250−260 μM, neither of the three ligands unwinds DNA to the extent induced by the classical intercalator EtBr at a concentration of only 2.5 μM. Thus, EtBr unwinds DNA at least 100 times more efficiently than any of the three protoberberine analogs. Further inspection of Figure 3 reveals that a DMC concentration of $\geq$260 μM is required to achieve the same approximate degree of unwinding induced by a DHDMC concentration of only 26 μM. Thus, DHDMC unwinds DNA at least 10 times more efficiently than DMC. Molecular modeling studies (data not shown) using MacroModel version 5.0 and the AMBER* force field (Mohamadi et al., 1990) reveal that, in contrast to the wholly unsaturated and essentially planar

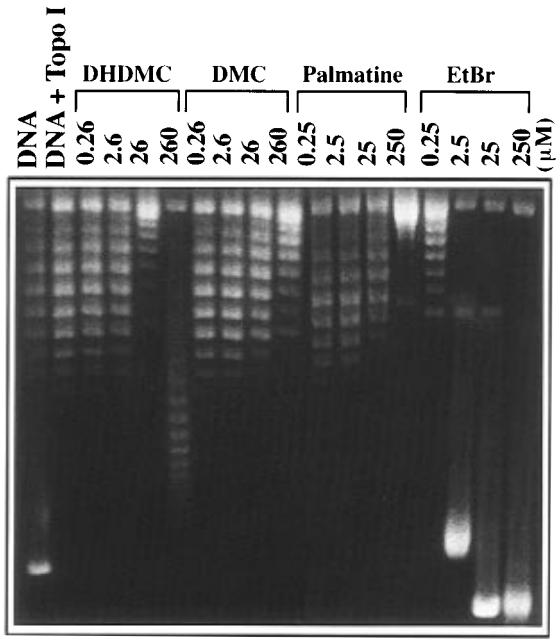

FIGURE 3: Agarose gel showing DNA duplex unwinding by the protoberberines and ethidium bromide (EtBr) in the presence of camptothecin-resistant human TOP1. The ligands and their concentrations are indicated at the tops of the lanes.

DMC molecule, the DHDMC molecule deviates from planarity, with the A-ring being tilted approximately 25° relative to the plane formed by rings C and D, due to saturation at the 5,6 positions of the B-ring (see Figure 1). Thus, the observation that DHDMC unwinds duplex DNA more efficiently than DMC is surprising, since one would expect the planar DMC molecule to intercalate more easily between base pairs than the nonplanar DHDMC molecule. In other words, on the basis of our DNA unwinding data, the protoberberine analogs do not "behave" like pure intercalators. In fact, fluorometric, viscometric, and NMR studies on berberine, which, like DHDMC, is saturated at the 5,6 positions of its B-ring, have been interpreted in terms of a model in which the ligand only partially intercalates into the DNA duplex (Davidson et al., 1977; Saran et al., 1995).

Note that the extent of DNA unwinding follows a hierarchy similar to that defined above based on our TOP1-mediated cleavage data, namely, DHDMC > DMC > palmatine. This correlation between DNA unwinding and TOP1 poisoning-based trends also extends to the hierarchy of overall DNA binding strength, which is presented in a later section.

Both DHDMC and DMC Exhibit Linear Dichroism Properties Consistent with at Least Some Degree of Intercalation. Flow linear dichroism is a useful technique for defining the mode by which a ligand is complexed with a host nucleic acid structure (Nordén, 1978; Nordén et al., 1992). Linear dichroism (LD) is defined by the relationship:

$$\mathrm{LD} = A_{\parallel} - A_{\perp} \qquad (1)$$

where $A_{\parallel}$ and $A_{\perp}$ denote respectively the sample absorbances with the polarization vectors of the light oriented in either a parallel or a perpendicular orientation with respect to the flow lines. When the transition dipole moment of a singly oriented chromophore (e.g., a DNA base and/or a bound aromatic ligand) lies within the plane of the molecule and makes an angle, θ, with the orientation axis, this angle can

be related to the LD value by the equation (Nordén, 1978; Wilson & Schellman, 1978; Geacintov et al., 1987; Nordén et al., 1992):

$$\mathrm{LD} = A\frac{3}{2}(3\cos^2\theta - 1)[F(G)] \qquad (2)$$

where A is the isotropic absorbance of the sample and $F(G)$ is an orientation factor, which has values in the range of $0 < F(G) < 1$. Equation 2 implies that a positive LD signal is associated with an angle θ of $<55°$, while a negative LD signal is associated with an angle θ of $>55°$. In a typical flow LD experiment, the long axis of the nucleic acid helix is aligned along the flow lines (Nordén, 1978; Wilson & Schellman, 1978; Geacintov et al., 1987; Nordén et al., 1992). Thus, the nucleic acid bases, which are oriented roughly perpendicular to the helix axis (i.e., $\theta_{\mathrm{bases}} \approx 90$ °C), give rise to a negative LD signal. A drug molecule that is bound to the minor groove of a nucleic acid structure typically exhibits an angle θ_{drug} of approximately 40−50° relative to the helix axis and therefore gives rise to a positive LD signal. In contrast to a minor groove-bound drug molecule, an intercalated drug molecule, like the nucleic acid bases, is oriented roughly perpendicular to the helix axis ($\theta_{\mathrm{drug}} \approx 90$ °C) and therefore gives rise to a negative LD signal.

Figure 4 shows the absorbance and LD spectra of salmon testes DNA when complexed with either DMC (panel A) or DHDMC (panel B) at a [base pair]/[total ligand] ratio of 5. Inspection of Figure 4 reveals that, as expected, the LD spectra of both ligand−DNA complexes are negative in the 240−300 nm wavelength region where the DNA absorbs. As observed for the LD spectra in this DNA-absorbing region, the LD spectra of both ligand−DNA complexes also are negative in the 300−380 nm ligand-absorbing wavelength region. These negative LD signals are consistent with DMC and DHDMC binding to duplex DNA via at least some degree of intercalation and, as such, are in accordance with our DNA unwinding measurements described above. By extension, it is reasonable to propose that palmatine binding to DNA also is intercalative in nature, since palmatine differs from DHDMC only by the position of a single methoxy group on the D-ring (see Figure 1) and, as discussed above (see Figure 3), unwinds duplex DNA.

DMC, DHDMC, and Palmatine Bind to and Enhance the Thermal Stabilities of the Alternating Copolymeric DNA Duplexes, Poly[d(A-T)]$_2$, Poly[d(I-C)]$_2$, and Poly[d(G-C)]$_2$. Panels A−C of Figure 5 show the UV melting curves for the poly[d(A-T)]$_2$ (panel A), poly[d(I-C)]$_2$ (panel B), and poly[d(G-C)]$_2$ (panel C) duplexes in the absence and presence of saturating amounts of DMC, DHDMC, and palmatine. Inspection of Figure 5 reveals that the presence of each of the three protoberberine analogs enhances the thermal stabilities of all three target DNA duplexes. These analog-induced changes in duplex thermal stability are consistent with all three ligands binding to each target duplex, with a preference for the duplex versus single-stranded state (Crothers, 1971; Snyder et al., 1989). Further inspection of Figure 5 reveals the extent of DMC-induced enhancement in duplex thermal stability to follow the hierarchy poly[d(G-C)]$_2$ > poly[d(A-T)]$_2$ > poly[d(I-C)]$_2$. Specifically, DMC binding increases the thermal stabilities of poly[d(G-C)]$_2$ (Figure 5C), poly[d(A-T)]$_2$ (Figure 5A), and poly[d(I-C)]$_2$ (Figure 5B) by approximately 11, 9, and 7 °C, respectively. In contrast to the behavior just described for DMC binding, the extent

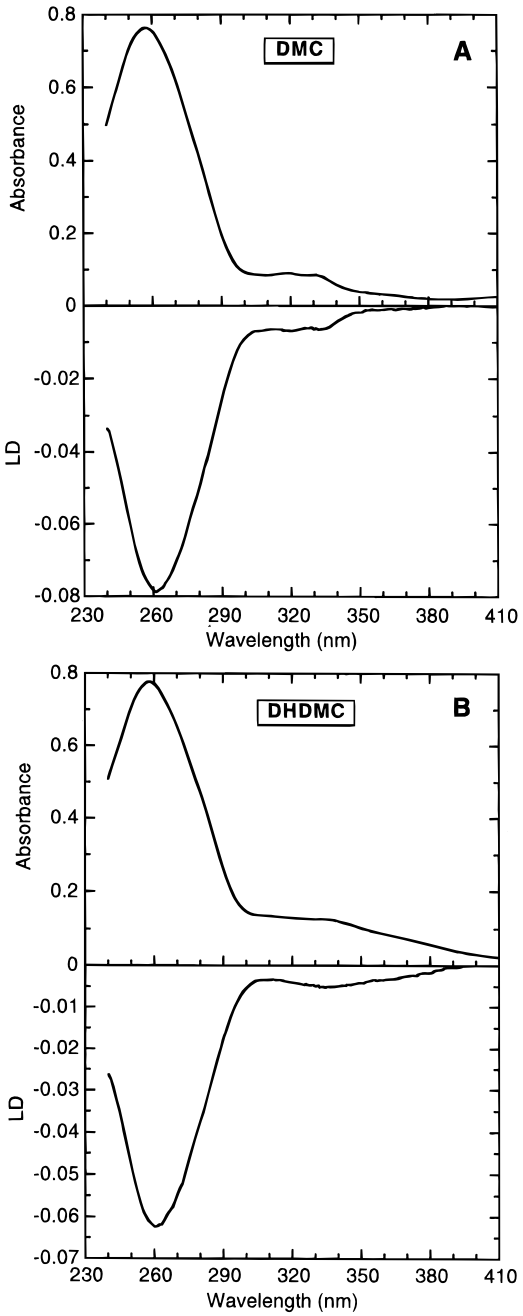

FIGURE 4: Isothermal absorbance and linear dichroism (LD) spectra at 25 °C for the salmon testes DNA complexes with DMC (A) and DHDMC (B) at a [total ligand] to [base pair] ratio (r_{bp}) of 0.2. Solution conditions were 10 mM sodium phosphate (pH 6.8) and 0.1 mM EDTA.

of DHDMC-induced enhancement in duplex thermal stability follows the hierarchy poly[d(A-T)]$_2$ > poly[d(I-C)]$_2$ > poly[d(G-C)]$_2$. Specifically, DHDMC binding increases the thermal stabilities of poly[d(A-T)]$_2$ (Figure 5A), poly[d(I-C)]$_2$ (Figure 5B), and poly[d(G-C)]$_2$ (Figure 5C) by approximately 23, 18, and 7 °C, respectively. Thus, as measured by differences in ΔT_{m}, these protoberberine analogs are able to distinguish between the different base sequences of the three target duplexes.

Note that, in contrast to both deoxyinosine and deoxyadenosine, deoxyguanosine contains a C2-amino group that protrudes into the minor groove of a DNA duplex. As a result of this key difference, which is the *sole* difference between deoxyguanosine and deoxyinosine residues, the poly[d(G-C)]$_2$ duplex contains a minor groove that is partially occluded by the C2-amino groups of the guanosine residues,

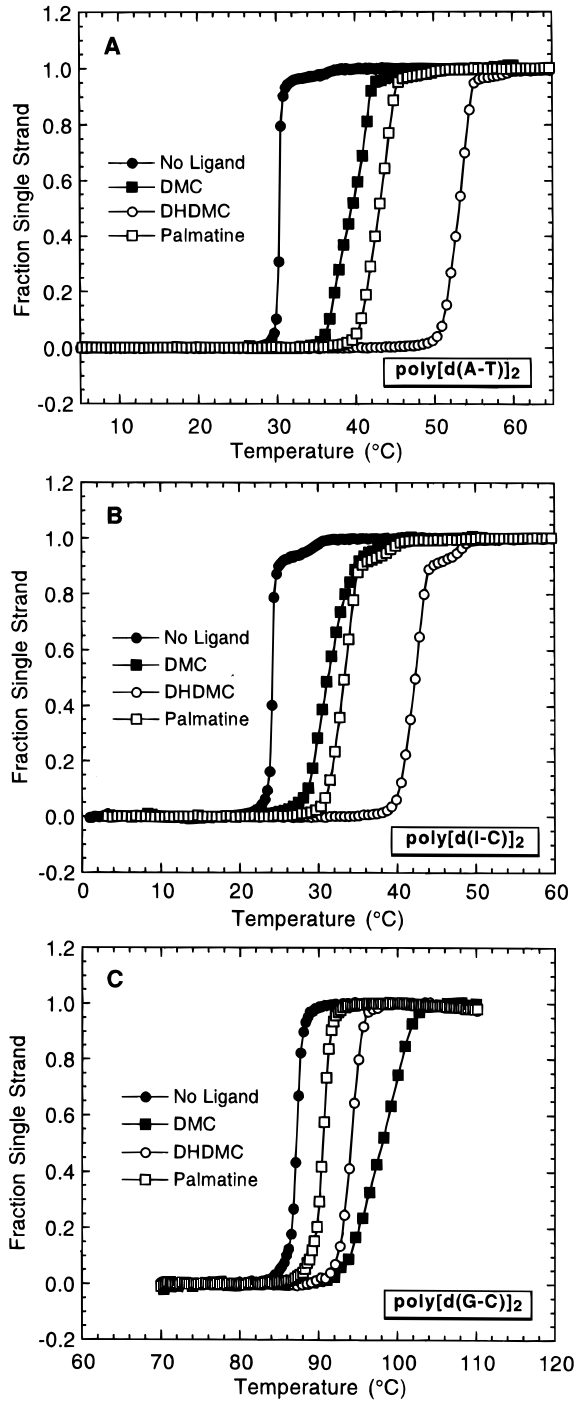

FIGURE 5: UV melting profiles for the poly[d(A-T)]$_2$ (A), poly-[d(I-C)]$_2$ (B), and poly[d(G-C)]$_2$ (C) duplexes (solid circles) and their complexes with DMC (solid squares), DHDMC (open circles), and palmatine (open squares) at a [total ligand] to [base pair] ratio (r_{bp}) of 0.5. Solution conditions were 2 mM sodium phosphate (pH 7.0) and 0.1 mM EDTA. For clarity of presentation, the melting curves were normalized by subtraction of the upper and lower base lines to yield plots of fraction of single strand versus temperature (Marky & Breslauer, 1987a). The melting profiles for poly[d(I-C)]$_2$ and its protoberberine complexes were acquired at 242 nm, while those for poly[d(A-T)]$_2$, poly[d(G-C)]$_2$, and their protoberberine complexes were acquired at 260 nm.

while both the poly[d(A-T)]$_2$ and poly[d(I-C)]$_2$ duplexes contain unobstructed minor grooves. Thus, the difference in hierarchy of ligand-induced changes in duplex thermal stability described above for DMC and DHDMC suggests that, in addition to discriminating between DNA duplexes with differing base sequences, the protoberberine analogs also are able to distinguish between duplexes with unobstructed and occluded minor grooves.

The extent of palmatine-induced enhancement in duplex thermal stability follows the same hierarchy as DHDMC; namely, poly[d(A-T)]$_2$ > poly[d(I-C)]$_2$ > poly[d(G-C)]$_2$. However, the magnitudes of palmatine-induced increases in duplex thermal stability are smaller than the corresponding increases noted above for DHDMC binding. Specifically, palmatine binding increases the thermal stabilities of poly-[d(A-T)]$_2$ (Figure 5A), poly[d(I-C)]$_2$ (Figure 5B), and poly-[d(G-C)]$_2$ (Figure 5C) by approximately 13, 9, and 3 °C, respectively. As noted above, palmatine differs from DHDMC by the position of a single methoxy group on the D-ring (see Figure 1). Thus, in addition to the sequence/structural properties of the target duplex, ligand structure also may play a role in modulating DNA recognition by protoberberines.

Relative DMC, DHDMC, and Palmatine Binding Affinities for the Poly[d(A-T)]$_2$, Poly[d(I-C)]$_2$, and Poly[d(G-C)]$_2$ Duplexes Derived from UV Melting Data. We used the ΔT_m method described below to assess the relative strength of protoberberine binding to the three polymeric DNA duplexes studied here. Measured ligand-induced changes in the thermal stabilities of the three polymeric DNA duplexes (see Figure 5) were used in conjunction with a 2 bp binding site size (n), characteristic of a nearest-neighbor exclusion mode of complexation, to estimate apparent ligand−DNA association constants at T_m (K_{T_m}) from the expression (Crothers, 1971):

$$\frac{1}{T_m^\circ} - \frac{1}{T_m} = \frac{R}{n(\Delta H_{WC})} \ln (1 + K_{T_m} L) \qquad (3)$$

where T_m° and T_m are the melting temperatures of the ligand-free and ligand-saturated duplexes, respectively; ΔH_{WC} is the enthalpy change for the melting of a Watson−Crick (WC) base pair in the absence of bound ligand (values we determined independently for the three target duplexes using DSC); and L is the free ligand concentration at T_m, which can be estimated by one-half the total ligand concentration. For meaningful comparisons, the calculated apparent binding constants at T_m should be extrapolated to a common reference temperature using the standard relationship:

$$\frac{\partial \ln K}{\partial (1/T)} = -\frac{\Delta H_b}{R} \qquad (4)$$

where ΔH_b is the enthalpy of ligand binding.

Table 1 summarizes the apparent association constants at 20 °C (K_{20}) that we have calculated using eqs 3 and 4 for DMC, DHDMC, and palmatine binding to the poly[d(A-T)]$_2$, poly[d(I-C)]$_2$, and poly[d(G-C)]$_2$ host duplexes. The DMC, DHDMC, and palmatine binding enthalpies required for extrapolation of the binding constants to a common reference temperature using eq 4 were determined for all the duplexes studied here using isothermal, stopped-flow mixing calorimetry. Figure 6 shows representative heat burst curves for the binding of DMC (panel A), DHDMC (panel B), and palmatine (panel C) to the poly[d(I-C)]$_2$ and poly[d(G-C)]$_2$ duplexes. The areas under these heat burst curves, as well as those for the binding of the three protoberberine analogs to the poly[d(A-T)]$_2$ duplex (not shown), were determined by integration to yield the heats of the binding reactions. The resulting ΔH_b values are listed in Table 2. It is

Table 1: ΔT_m-Derived Binding Affinities of DMC, DHDMC, and Palmatine for the Three Polymeric DNA Duplexes at 20 °C[a]

ligand	target duplex	$T_m°$ [b] (°C)	T_m [b] (°C)	K_{20} [c] (M^{-1})
DMC	poly[d(A-T)]$_2$	30.4 ± 0.1	39.6 ± 0.1	(3.9 ± 0.2) × 10^5
DMC	poly[d(I-C)]$_2$	24.1 ± 0.2	31.4 ± 0.2	(2.9 ± 0.2) × 10^5
DMC	poly[d(G-C)]$_2$	87.3 ± 0.1	97.9 ± 0.3	(8.8 ± 1.3) × 10^5
DHDMC	poly[d(A-T)]$_2$	30.4 ± 0.1	52.9 ± 0.3	(34 ± 3.4) × 10^5
DHDMC	poly[d(I-C)]$_2$	24.1 ± 0.2	41.9 ± 0.2	(18 ± 1.6) × 10^5
DHDMC	poly[d(G-C)]$_2$	87.3 ± 0.1	94.1 ± 0.1	(5.6 ± 1.1) × 10^5
palmatine	poly[d(A-T)]$_2$	30.4 ± 0.1	43.2 ± 0.2	(7.4 ± 0.6) × 10^5
palmatine	poly[d(I-C)]$_2$	24.1 ± 0.2	33.4 ± 0.1	(4.5 ± 0.3) × 10^5
palmatine	poly[d(G-C)]$_2$	87.3 ± 0.1	90.4 ± 0.3	(1.5 ± 0.4) × 10^5

[a] Solution conditions were 2 mM sodium phosphate (pH 7.0) and 0.1 mM EDTA. [b] T_m values were derived from UV melting profiles at 15 μM base pair (bp) in the absence ($T_m°$) and presence of ligand at a [total ligand] to [base pair] ratio (r_{bp}) of 0.5. Each T_m value is an average derived from at least two independent experiments, with the indicated errors corresponding to the standard deviation from the mean. [c] Binding constants at 20 °C (K_{20}) were determined using eqs 3 and 4, the appropriate values of ΔH_b listed in Table 2, and the following calorimetrically determined (see Materials and Methods) duplex-to-single strand transition enthalpies (ΔH_{WC}) for the three host polymeric duplexes: 8.3 kcal/mol bp for poly[d(A-T)]$_2$; 8.7 kcal/mol bp for poly[d(I-C)]$_2$; and 12.6 kcal/mol bp for poly[d(G-C)]$_2$. The indicated uncertainties reflect the maximum errors in K_{20} that result from the corresponding uncertainties noted above in T_m, $T_m°$, and ΔH_b, as propagated through eqs 3 and 4.

interesting to compare these enthalpies for protoberberine binding with those previously reported (Marky et al., 1983a,b, 1985; Breslauer et al., 1987, 1988; Chou et al., 1987; Marky & Breslauer, 1987b; Chou, 1990) for the binding of EtBr, a classic DNA intercalator, to the poly[d(A-T)]$_2$, poly[d(I-C)]$_2$, and poly[d(G-C)]$_2$ duplexes (−10.0, −9.2, and −6.3 kcal/mol, respectively), as well as for the binding of netropsin, a classic minor groove binder, to the poly[d(A-T)]$_2$ and poly[d(I-C)]$_2$ duplexes (−11.2 and −9.9 kcal/mol, respectively). This comparison reveals that the enthalpies of DMC, DHDMC, and palmatine binding to the poly[d(A-T)]$_2$, poly[d(I-C)]$_2$, and/or poly[d(G-C)]$_2$ host duplexes, which range from −0.8 to −4.6 kcal/mol, are significantly less exothermic (less favorable) than the corresponding binding enthalpies of either EtBr or netropsin. In other words, on the basis of the binding enthalpy data, the protoberberine analogs do not behave like pure intercalators or pure minor groove binders, an observation in accordance with the DNA unwinding data described above.

Inspection of the data in Table 1 reveals that the apparent binding affinities of DMC follow the hierarchy poly[d(G-C)]$_2$ > poly[d(A-T)]$_2$ > poly[d(I-C)]$_2$. By contrast with this binding hierarchy for DMC, the apparent binding affinities of DHDMC and palmatine follow the hierarchy poly[d(A-T)]$_2$ > poly[d(I-C)]$_2$ > poly[d(G-C)]$_2$. Thus, DMC preferentially binds to a duplex whose minor groove is partially occluded by guanine C2-amino groups, while DHDMC and palmatine preferentially bind to duplexes with unobstructed minor grooves. Note the agreement between the hierarchies of apparent protoberberine binding affinities and those noted above for binding-induced enhancement in duplex thermal stability. Hence, given the binding enthalpies listed in Table 2, the relative extent to which either of the three protoberberine analogs thermally stabilizes a target duplex is correlated with its relative binding affinity.

Further inspection of the data in Table 1 reveals that all three protoberberine analogs bind to the poly[d(A-T)]$_2$ duplex with a higher affinity than they bind to the poly[d(I-C)]$_2$ duplex. Comparison of these data with those in Table 2 reveals this protoberberine binding preference to be enthalpic in origin. Both the poly[d(A-T)]$_2$ and poly[d(I-C)]$_2$ host duplexes possess similar global structures and accessible minor grooves lined by identical functional groups (Arnott et al., 1974; Remeta et al., 1993). Thus, the protoberberine preference for binding the poly[d(A-T)]$_2$ relative to the poly[d(I-C)]$_2$ host duplex may reflect differences in the ligand−base stacking energies between the two ligand−duplex complexes.

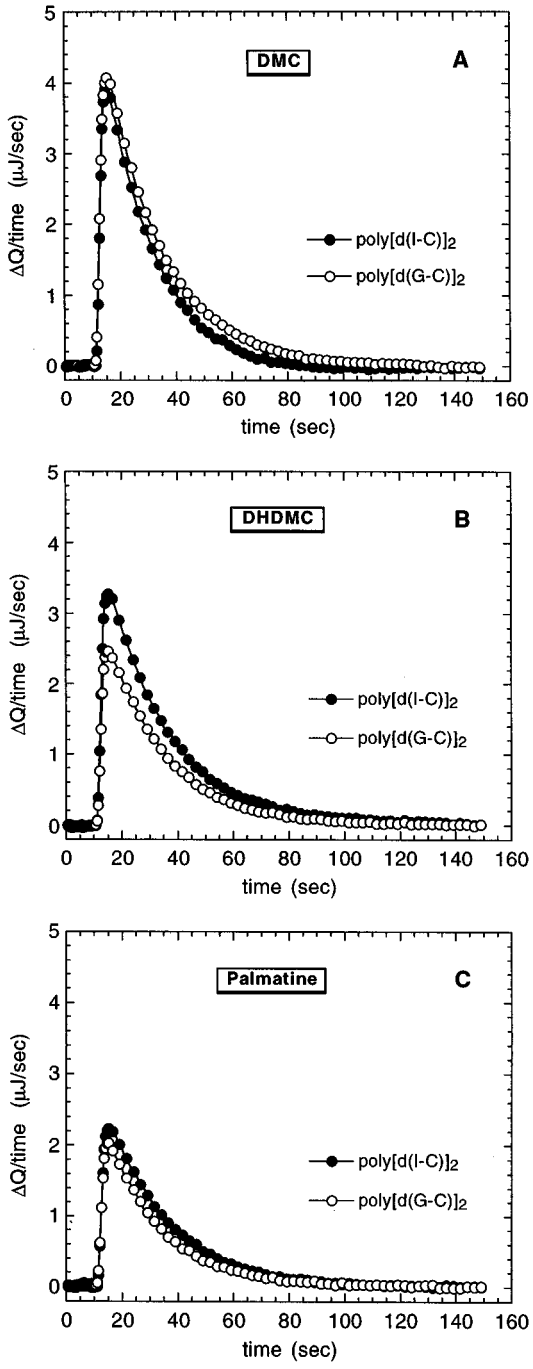

FIGURE 6: Isothermal, stopped-flow calorimetric heat burst curves at 20 °C for the complexation of poly[d(I-C)]$_2$ (solid circles) and poly[d(G-C)]$_2$ (open circles) with DMC (A), DHDMC (B), and palmatine (C). Solution conditions were as described in the legend to Figure 5.

DISCUSSION

Protoberberines Exhibit both Intercalative and Minor Groove Binding Properties When Complexed with Duplex

Table 2: Calorimetrically Derived Binding Enthalpies (ΔH_b) for the Interactions of DMC, DHDMC, and Palmatine with the Three Polymeric DNA Duplexes at 20 °C[a]

ligand	target duplex	ΔH_b[b] (kcal/mol)
DMC	poly[d(A-T)]$_2$	-1.6 ± 0.2
DMC	poly[d(I-C)]$_2$	-0.8 ± 0.1
DMC	poly[d(G-C)]$_2$	-1.8 ± 0.2
DHDMC	poly[d(A-T)]$_2$	-4.6 ± 0.3
DHDMC	poly[d(I-C)]$_2$	-3.9 ± 0.3
DHDMC	poly[d(G-C)]$_2$	-2.4 ± 0.4
palmatine	poly[d(A-T)]$_2$	-2.4 ± 0.3
palmatine	poly[d(I-C)]$_2$	-2.1 ± 0.3
palmatine	poly[d(G-C)]$_2$	-1.5 ± 0.2

[a] Solution conditions are as described in Table 1. [b] ΔH_b values were determined at a [total ligand] to [base pair] ratio (r_{bp}) of 0.5, with the indicated uncertainties corresponding to the sum of the standard errors from two separate mixing experiments (DNA−ligand and ligand−buffer) of at least 14 independent injections each.

DNA. As noted above, the observation that protoberberine binding induces both DNA unwinding (Figure 3) and negative ligand LD signals (Figure 4) is consistent with protoberberine binding to duplex DNA via at least some degree of intercalation. However, the enhanced DNA unwinding properties exhibited by the 5,6-saturated, nonplanar DHDMC ligand relative to the 5,6-unsaturated, planar DMC molecule suggest that the protoberberines do not behave like classic intercalators. The nonclassical nature by which the protoberberines intercalate into duplex DNA also is evident in the binding enthalpy data listed in Table 2, which reveal that the enthalpy of protoberberine binding to duplex DNA is significantly less exothermic (favorable) than that previously reported (Chou et al., 1987; Chou, 1990) for the duplex binding of the classic intercalators, EtBr and propidium iodide. In addition to the evidence just cited for a nonclassically intercalative mode of protoberberine binding to duplex DNA, our UV melting (Figure 5) and DNA binding (Table 1) data indicate that the protoberberine analogs are able to distinguish between DNA duplexes with unobstructed or open minor grooves {e.g., poly[d(A-T)]$_2$ and poly[d(I-C)]$_2$} and those whose minor grooves are occluded {e.g., poly[d(G-C)]$_2$}. In the aggregate, the observations described above are consistent with a mode of protoberberine binding to DNA that exhibits properties characteristic of both intercalation and a minor groove-directed interaction. One possible model to describe the protoberberine−DNA interaction is a mixed-mode binding model in which the ligand partially intercalates into the DNA duplex, with the nonintercalated portion of the ligand molecule protruding into the minor groove, where it is available for interactions with the atoms lining the floor and/or walls of the minor groove. A partial intercalation binding model has previously been proposed to describe the binding of berberine to duplex DNA (Davidson et al., 1977; Saran et al., 1995). Our mixed-mode binding model presented here extends this partial intercalation model to include an interaction between the nonintercalated portion of the protoberberine ligand and the minor groove of the host duplex.

Comparison of DMC with DHDMC: Saturation of the 5−6 Double Bond in the B-Ring Is Associated with Preferential Binding to DNA Duplexes with Unobstructed Minor Grooves and Enhanced TOP1 Poisoning. A comparison of the DNA binding data (see Table 1) for DMC and DHDMC reveals that DMC preferentially binds to the duplex with the occluded minor groove {poly[d(G-C)]$_2$} relative to the duplexes with accessible minor grooves {poly[d(A-T)]$_2$ and poly[d(I-C)]$_2$}. By contrast, DHDMC preferentially binds to the poly[d(A-T)]$_2$ and poly[d(I-C)]$_2$ duplexes relative to the poly[d(G-C)]$_2$ duplex. Thus, saturation of the 5−6 double bond in the B-ring of DMC, thereby converting DMC to DHDMC (see Figure 1), reverses the binding preference of DMC from the host duplex with the occluded minor groove to the host duplexes with unobstructed minor grooves. This reversal of binding preference is the product of approximately 9- and 6-fold enhancements of affinity for the poly[d(A-T)]$_2$ and poly[d(I-C)]$_2$ duplexes, respectively, as well as a 1.5-fold reduction in affinity for the poly[d(G-C)]$_2$ duplex. Thus, the reversal in DNA binding preference accompanying saturation of the 5−6 double bond in the B-ring of DMC is due to both an enhanced affinity for duplexes with open minor grooves and a reduced affinity for duplexes with occluded minor grooves. As noted above, molecular modeling studies (data not shown) using MacroModel version 5.0 and the AMBER* force field (Mohamadi et al., 1990) reveal that DMC is an essentially planar molecule. By contrast, DHDMC deviates from planarity, with the plane of the A-ring being tilted by approximately 25° relative to the plane formed by rings C and D. This degree of ring tilting is in relatively good agreement with the values of 10−16° previously reported in crystallographic studies (Abdol Abadi et al., 1984; Kariuki & Jones, 1995) on berberine, which, like DHDMC, is saturated at the 5,6 positions of its B-ring. Thus, saturation of the 5−6 double bond in the B-ring induces a tilt in the ligand molecule that does not exist when the 5,6 positions are unsaturated. This tilting at the B-ring may serve to facilitate interactions (e.g., van der Waals contacts) between the nonintercalated portion of the protoberberine molecule and atoms lining the floor and/or walls of the DNA minor groove. On the basis of our drug modeling and DNA binding studies, we propose a mixed-mode DNA binding model for protoberberine analogs in which rings C and D are intercalated into the helical stack, while ring A protrudes into the minor groove. The intercalative and minor groove-directed components of the protoberberine analogs are schematically depicted in Figure 7. In such a mixed-mode DNA binding model, saturation at the 5,6 positions of the B-ring tilts the A-ring ~25° relative to the plane formed by rings C and D, thereby promoting favorable interactions between atoms on the A-ring and atoms lining the floor and/or walls of the DNA minor groove. Such ligand−DNA interactions would necessitate the ligand having unhindered access to the minor groove of the host duplex, a necessity that would be manifested by a preferential

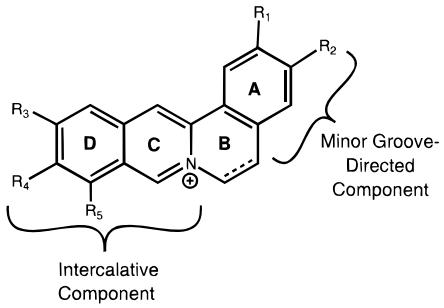

FIGURE 7: Schematic representation of the intercalative and minor groove-directed components of a protoberberine molecule, as invoked by the "mixed-mode" DNA binding model described in the text. The various sites of modification on rings A, B, and D of the three protoberberines studied here are indicated either by an R_n notation (rings A and D) or by a dashed line (ring B).

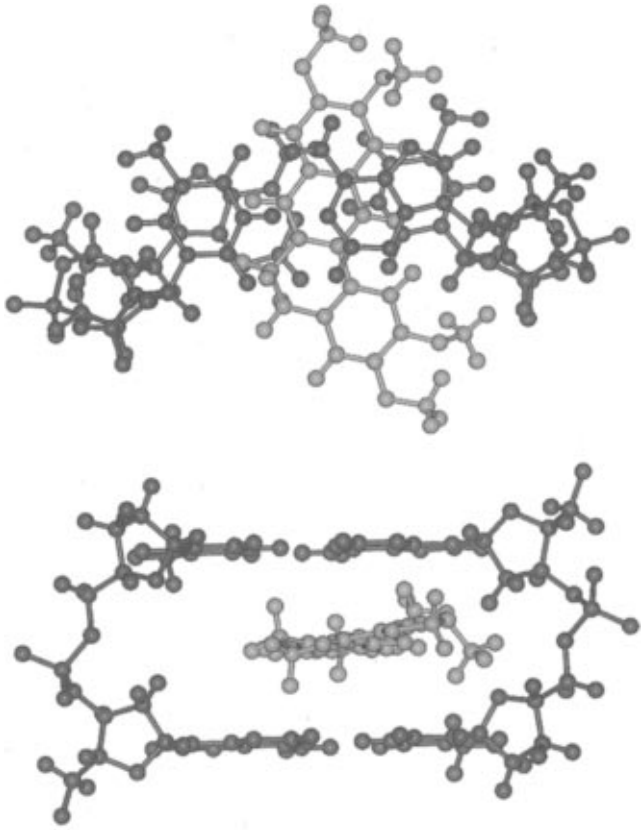

FIGURE 8: Low-energy model for the DHDMC−poly[d(A-T)]$_2$ complex. The DNA is shown in purple, while the DHDMC molecule is shown in red. (Top) View looking down the helical axis of the host DNA duplex. The upper and lower edges of the DNA in this view correspond to the major and minor grooves, respectively. (Bottom) Side view looking into the DNA minor groove.

binding to DNA duplexes with unobstructed minor grooves, as noted above for DHDMC. Furthermore, it is likely that, in addition to enhancing interactions between the minor groove of the host duplex and the A-ring of the ligand, tilting at the B-ring also would, to some extent, be detrimental to the stacking interactions between the DNA bases and the intercalated component (rings C and D) of the protoberberine ligand (see Figure 7). This reduction in the extent of base−ligand stacking may account for the lower observed affinity of DHDMC for the poly[d(G-C)]$_2$ duplex than that exhibited by DMC (see Table 1).

To gain insight into the potential structural nature of a protoberberine−DNA complex, we used the computer modeling methods described in Materials and Methods to explore energetically feasible structures that the DHDMC−poly[d(A-T)]$_2$ complex might adopt. Figure 8 shows both top (looking down the helix axis) and side (looking into the minor groove) views of one of the lower energy structures to emerge from these studies. Inspection of the top view in Figure 8 reveals a structure in which rings C and D of the ligand are stacked between adjacent A·T base pairs in an orientation that is almost perpendicular to the long axis of the adenine bases. A second feature of this structure revealed by the top view in Figure 8 is the protrusion of the ligand A-ring into the DNA minor groove. Note that the two methoxy groups on the A-ring are twisted above and below the plane of the ring. Molecular modeling studies (not shown) on the *DNA-free* state of DHDMC using the MacroModel version 5.0 and the AMBER* force field (Mohamadi et al., 1990) indicate that the two methoxy groups adopt this twisted structure to minimize the sterically unfavorable interactions that arise from their *ortho* positioning on the ring, an observation in agreement with previous crystallographic studies on berberine (Abdol Abadi et al., 1984; Kariuki & Jones, 1995), which, like DHDMC, contains two *ortho*-substituted methoxy moieties. Inspection of the side view in Figure 8 reveals the positive tilt of the minor groove-directed A-ring relative to the plane formed by the intercalated C- and D-ring. This tilting of the A-ring allows the minor groove of the host duplex to accommodate the twisted structure adopted by the two *ortho*-substituted methoxy groups, while also positioning the 2-methoxy group for favorable van der Waals contacts with backbone sugar atoms lining the minor groove. This structural model suggests that attractive van der Waals interactions between the host duplex and *both* the intercalated and minor groove-directed portions of the ligand may contribute to the stability of the DHDMC−poly[d(A-T)]$_2$ complex.

Our DNA cleavage data (Figure 2A) reveal that DHDMC is a 100-fold more potent stimulator of TOP1-mediated DNA cleavage than DMC. Thus, saturation of the 5−6 double bond in the B-ring of DMC not only reverses its DNA binding preference from host duplexes with occluded minor grooves to host duplexes with unobstructed minor grooves, as noted above, but also converts it from a weak to a strong TOP1 poison. In other words, the ability of a protoberberine analog to poison TOP1 is correlated with its preferential binding to duplexes with accessible minor grooves. This correlation implies that an interaction between the protoberberine analog and the minor groove of the host DNA duplex is important for TOP1 poisoning. Recall our mixed-mode DNA binding model, detailed above, which invokes the partial intercalation of the protoberberine molecule (by rings C and D) into the helical stack, with the nonintercalated portion (ring A) protruding into and interacting with the minor groove (see Figures 7 and 8). Our DNA cleavage data suggest that the minor groove-directed interaction of the nonintercalated portion of the ligand is crucial for TOP1 poisoning. A correlation between minor groove-directed ligand−DNA interactions and TOP1 poisoning may not be restricted to the protoberberine family of compounds. Numerous other mixed-mode DNA binding ligands, including actinomycin D, morpholinyldoxorubicin, nogalamycin, and indolocarbazole derivatives such as ED-110, have been shown to be potent TOP1 poisons (Trask & Muller, 1988; Wassermann et al., 1990; Yamashita et al., 1992; Chen et al., 1993b; Yoshinari et al., 1993; Chen & Liu, 1994). Our results presented here suggest that the DNA minor groove-directed portions of these drug molecules may be critical to their TOP1 poisoning activities. In fact, the intercalative binding component may not be necessary if the minor groove-directed interaction is sufficiently strong. In this connection, recent studies have shown that minor groove binders, such as the bi- and terbenzimidazole families of compounds, also exhibit potent TOP1 poisoning activities (Chen et al., 1993a,b; Sun et al., 1994, 1995; Kim et al., 1996a).

Comparison of DHDMC with Palmatine: Transferring a Methoxy Group from the 11 to the 9 Position of the D-Ring in a Protoberberine Molecule Whose 5,6 Positions Are Saturated Is Associated with a Reduction in DNA Binding Affinity and Reduced TOP1 Poisoning. A comparison of the DNA binding data (see Table 1) for DHDMC and palmatine reveals that DHDMC binds to the three host

polymeric DNA duplexes with an approximately 4−5-fold higher affinity than does palmatine. In other words, the transfer of a single methoxy group from the 11 to the 9 position of the D-ring in DHDMC, thereby converting DHDMC to palmatine (see Figure 1), reduces the overall duplex DNA binding affinity of DHDMC by approximately 4−5-fold. This observation is consistent with our mixed-mode DNA binding model because it suggests that the intercalated rather than the minor groove-directed portion of the ligand molecule is being affected by the methoxy group transfer, since a change in the structure of the minor groove-directed portion of the ligand is more likely to affect differentially the host duplexes with accessible minor grooves {poly[d(A-T)]$_2$ and poly[d(I-C)]$_2$} versus the host duplex with the occluded minor groove {poly[d(G-C)]$_2$}. Furthermore, this observation supports our assignment of rings C and D to that portion of the protoberberine molecule which intercalates between base pairs of the host duplex. The reduction in the DNA binding affinity of DHDMC as a result of the methoxy group transfer suggests that a 10,11-dimethoxy substitution of the D-ring may be more sterically compatible with the structural geometry of the duplex intercalation site than a 9,10-dimethoxy substitution. Crystallographic studies (Abdol Abadi et al., 1984; Kariuki & Jones, 1995) on berberine, which, like palmatine, contains a 9,10-dimethoxy substitution on its D-ring, indicate that the two methoxy groups are twisted above and below the plane formed by rings C and D, with the methoxy group at the 9 position being displaced by ≈0.1 Å below the C−D plane and the methoxy group at the 10 position being displaced by ≈0.3 Å above the C−D plane. These displacements of the bulky methoxy groups from the C−D plane may sterically interfere with proper insertion of the C- and D-rings between base pairs, thereby diminishing the extent of ligand−base stacking and, ultimately, reducing duplex binding affinity.

Our DNA cleavage data (Figure 2A) reveal that DHDMC is a potent stimulator of TOP1-mediated DNA cleavage, while palmatine does not stimulate TOP1-mediated DNA cleavage above background levels. Thus, the reduction in duplex binding affinity that accompanies the transfer of a methoxy group from the 11 to the 9 position of the D-ring in DHDMC is correlated with a corresponding reduction in TOP1 poisoning activity. In other words, despite possessing a 5,6-saturated B-ring, which should favor TOP1 poisoning by virtue of an enhanced A-ring interaction with the minor groove of the host duplex, palmatine still fails to poison TOP1 because of the offsetting disruptive effect of the 9,10-dimethoxy substituted D-ring on the intercalative component of the ligand−duplex complex.

Correlation between a Minor Groove-Directed Ligand−DNA Interaction and TOP1 Poisoning. The importance of a minor groove-directed interaction in TOP1 poisoning by protoberberines as well as other TOP1 poisons contrasts with the known correlation between intercalative DNA binding and the poisoning of TOP2 (Liu, 1989). Intercalative DNA binding has been shown to be necessary but not sufficient for TOP2 poisoning by DNA intercalating antitumor drugs (Liu, 1989). Similarly, minor groove binding alone is necessary but not sufficient for TOP1 poisoning by DNA minor groove-directed ligands (Chen et al., 1993b). It is likely that both drug−DNA and drug−enzyme interactions are important for the stabilization of TOP−DNA−drug ternary cleavable complexes. The dichotomy of DNA binding modes in differential topoisomerase poisoning may reflect the fundamental differences in enzyme catalysis by the type I and type II DNA topoisomerases. Closure of a topological domain surrounding the cleavage site by the TOP2 homodimer, due to two symmetrical protein−DNA contacts, has been proposed as the molecular mechanism by which DNA intercalating ligands poison TOP2 (the "misalignment" model) (D'Arpa & Liu, 1989). However, it is unlikely that TOP1 is able to close a topological domain surrounding the cleavage site, since doing so would prevent it from sensing the writhe of the DNA via a single nick (swivel) (Andersen et al., 1994). Because the nick functions like a swivel, the unwinding of DNA induced by the binding of intercalators would not be expected to cause the misalignment of the two transiently broken DNA termini. Consequently, the intercalative mode of DNA binding is not likely to be involved directly in TOP1 poisoning. For the protoberberines studied here, the intercalative portion of the "mixed" binding mode may serve to stabilize the minor groove-directed interaction that is primarily responsible for poisoning TOP1. The molecular mechanism of TOP1 poisoning via a minor groove-directed ligand−DNA interaction is unclear. Ligand-induced DNA bending, which, in turn, causes the transiently cleaved DNA termini to become misaligned, has been suggested as a possible mechanism by which minor groove binding ligands poison TOP1 (Chen et al., 1993b; Chen & Liu, 1994). Additional studies are required to establish the role of DNA minor groove-directed interactions in TOP1 poisoning by protoberberines as well as by other TOP1-poisoning compounds.

ACKNOWLEDGMENT

We are indebted to Dr. Tongming Liu and Mr. Zhitao Xu for their assistance with the acquisition and analysis of the linear dichroism data.

REFERENCES

Abdol Abadi, B. E., Moss, D. S., & Palmer, R. A. (1984) *J. Crystallogr. Spectrosc. Res. 14*, 269−281.

Andersen, A. H., Svejstrup, J. Q., & Westergaard, O. (1994) *Adv. Pharmacol. 29A*, 83−101.

Arnott, S., Chandrasekaran, R., Hukins, D. W. L., Smith, P. J. C., & Watts, L. (1974) *J. Mol. Biol. 88*, 523−533.

Bauer, W., & Vinograd, J. (1968) *J. Mol. Biol. 33*, 141−171.

Berman, H. M., & Young, P. R. (1981) *Annu. Rev. Biophys. Bioeng. 10*, 87−114.

Bodley, A. L., Liu, L. F., Israel, M., Ramakrishnan, S., Yoshihiro, K., Giuliani, F. C., Kirschenbaum, S., Silber, R., & Potmesil, M. (1989) *Cancer Res. 49*, 5969−5978.

Breslauer, K. J., Remeta, D. P., Chou, W.-Y., Ferrante, R., Curry, J., Zaunczkowski, D., Snyder, J. G., & Marky, L. A. (1987) *Proc. Natl. Acad. Sci. U.S.A. 84*, 8922−8926.

Breslauer, K. J., Ferante, R., Marky, L. A., Dervan, P. B., & Youngquist, R. S. (1988) in *Structure & Expression, Volume 2: DNA and Its Drug Complexes* (Sarma, R. H., & Sarma, M. H., Eds.) pp 273−290, Adenine Press, Schenectady, NY.

Chandrasekaran, R., & Arnott, S. (1989) in *Landolt-Börnstein Numerical Data and Functional Relationships in Science and Technology, Group VII/1b, Nucleic Acids* (Saenger, W., Ed.) pp 31−170, Springer-Verlag, Berlin.

Chen, A. Y., & Liu, L. F. (1994) *Annu. Rev. Pharmacol. Toxicol. 34*, 191−218.

Chen, A. Y., Yu, C., Bodley, A., Peng, L. F., & Liu, L. F. (1993a) *Cancer Res. 53*, 1332−1337.

Chen, A. Y., Yu, C., Gatto, B., & Liu, L. F. (1993b) *Proc. Natl. Acad. Sci. U.S.A. 90*, 8131−8135.

Chou, W.-Y. (1990) Ph.D. Thesis, Rutgers University, New Brunswick, NJ.

Chou, W. Y., Marky, L. A., Zaunczkowski, D., & Breslauer, K. J. (1987) *J. Biomol. Struct. Dyn. 5*, 345−359.
Clark, G. R., Gray, E. J., Neidle, S., Li, Y.-H., & Leupin, W. (1996) *Biochemistry 35*, 13745−13752.
Crawford, L. V., & Waring, M. J. (1967) *J. Mol. Biol. 25*, 23−30.
Crothers, D. M. (1971) *Biopolymers 10*, 2147−2160.
D'Arpa, P., & Liu, L. F. (1989) *Biochim. Biophys. Acta 989*, 163−177.
Davidson, M. W., Lopp, I., Alexander, S., & Wilson, W. D. (1977) *Nucleic Acids Res. 4*, 2697−2712.
Debnath, D., Kumar, G. S., & Maiti, M. (1991) *J. Biomol. Struct. Dyn. 9*, 61−79.
Fede, A., Labhardt, A., Bannwarth, W., & Leupin, W. (1991) *Biochemistry 30*, 11377−11388.
Fede, A., Billeter, M., Leupin, W., & Wüthrich, K. (1993) *Structure 1*, 177−186.
Fujii, N., Yamashita, Y., Saitoh, Y., & Nakano, H. (1993) *J. Biol. Chem. 268*, 13160−13165.
Gatto, B., Sanders, M. M., Yu, C., Wu, H.-Y., Makhey, D., LaVoie, E. J., & Liu, L. F. (1996) *Cancer Res. 56*, 2795−2800.
Geacintov, N. E., Ibanez, V., Rougée, M., & Bensasson, R. V. (1987) *Biochemistry 26*, 3087−3092.
Gulbransen, E. A., & Robinson, A. L. (1934) *J. Am. Chem. Soc. 56*, 2637−2641.
Hertzberg, R. P., Busby, R. W., Caranfa, M. J., Holden, K. G., Johnson, R. K., Hecht, S. M., & Kingsbury, W. D. (1990) *J. Biol. Chem. 265*, 19287−19295.
Hsiang, Y.-H., Hertzberg, R., Hecht, S., & Liu, L. F. (1985) *J. Biol. Chem. 260*, 14873−14878.
Hsiang, Y.-H., Liu, L. F., Wall, M. E., Wani, M. C., Nicholas, A. W., Manikumar, G., Kirschenbaum, S., Silber, R., & Potmesil, M. (1989) *Cancer Res. 49*, 4385−4389.
Kanzawa, F., Nishio, K., Kubota, N., & Saijo, N. (1995) *Cancer Res. 55*, 2806−2813.
Kariuki, B. M., & Jones, W. (1995) *Acta Crystallogr. C51*, 1234−1240.
Keller, W. (1975) *Proc. Natl. Acad. Sci. U.S.A. 72*, 4876−4880.
Kim, J. S., Gatto, B., Yu, C., Liu, A., Liu, L. F., & LaVoie, E. J. (1996a) *J. Med. Chem. 39*, 992−998.
Kim, J. S., Sun, Q., Gatto, B., Yu, C., Liu, A., Liu, L. F., & LaVoie, E. J. (1996b) *Bioorg. Med. Chem. 4*, 621−630.
Leteurtre, F., Fujimori, A., Tanizawa, A., Chhabra, A., Mazumder, A., Kohlhagen, G., Nakano, H., & Pommier, Y. (1994) *J. Biol. Chem. 269*, 28702−28707.
Liu, L. F. (1989) *Annu. Rev. Biochem. 58*, 351−375.
Makhey, D., Gatto, B., Yu, C., Liu, A., Liu, L. F., & LaVoie, E. J. (1995) *Med. Chem. Res. 5*, 1−12.
Makhey, D., Gatto, B., Yu, C., Liu, A., Liu, L. F., & LaVoie, E. J. (1996) *Bioorg. Med. Chem. 4*, 781−791.
Marky, L. A., & Breslauer, K. J. (1987a) *Biopolymers 26*, 1601−1620.
Marky, L. A., & Breslauer, K. J. (1987b) *Proc. Natl. Acad. Sci. U.S.A. 84*, 4359−4363.
Marky, L. A., Snyder, J. G., & Breslauer, K. J. (1983a) *Nucleic Acids Res. 11*, 5701−5715.
Marky, L. A., Snyder, J. G., Remeta, D., & Breslauer, K. J. (1983b) *J. Biomol. Struct. Dyn. 1*, 487−507.
Marky, L. A., Curry, J., & Breslauer, K. J. (1985) in *Molecular Basis of Cancer, Part B: Macromolecular Recognition, Chemotherapy, and Immunology* (Rein, R., Ed.) pp 155−173, Alan R. Liss, Inc., New York.
Mohamadi, F., Richards, N. G. J., Guida, W. C., Liskamp, R., Lipton, M., Caufield, C., Chang, G., Hendrickson, T., & Still, W. C. (1990) *J. Comput. Chem. 11*, 440−467.
Mudd, C. P., & Berger, R. L. (1988) *J. Biochem. Biophys. Methods 17*, 171−192.
Müller, W., & Crothers, D. M. (1968) *J. Mol. Biol. 35*, 251−290.
Nordén, B. (1978) *Appl. Spectrosc. Rev. 14*, 157−248.
Nordén, B., Kubista, M., & Kurucsev, T. (1992) *Q. Rev. Biophys. 25*, 51−170.
Parkinson, J. A., Barber, J., Douglas, K. T., Rosamond, J., & Sharples, D. (1990) *Biochemistry 29*, 10181−10190.
Pilch, D. S., Kirolos, M. A., Liu, X., Plum, G. E., & Breslauer, K. J. (1995) *Biochemistry 34*, 9962−9976.
Pilch, D. S., Xu, Z., Sun, Q., LaVoie, E. J., Liu, L. F., Geacintov, N. E., & Breslauer, K. J. (1996) *Drug Des. Discovery 13* (3−4), 115−133.
Pjura, P. E., Grzeskowiak, K., & Dickerson, R. E. (1987) *J. Mol. Biol. 197*, 257−271.
Poddevin, B., Riou, J.-F., Lavelle, F., & Pommier, Y. (1993) *Mol. Pharmacol. 44*, 767−774.
Poltev, V. I., & Shulyupina, N. V. (1986) *J. Biomol. Struct. Dyn. 3*, 739−765.
Pommier, Y., Kohlhagen, G., Kohn, K. W., Leteurtre, F., Wani, M. C., & Wall, M. E. (1995) *Proc. Natl. Acad. Sci. U.S.A. 92*, 8861−8865.
Porter, S. E., & Champoux, J. J. (1989) *Nucleic Acids Res. 17*, 8521−8532.
Potmesil, M., & Pinedo, H. (1995) *Camptothecins: New Anticancer Agents*, CRC Press, Boca Raton, FL.
Remeta, D. P., Mudd, C. P., Berger, R. L., & Breslauer, K. J. (1991) *Biochemistry 30*, 9799−9809.
Remeta, D. P., Mudd, C. P., Berger, R. L., & Breslauer, K. J. (1993) *Biochemistry 32*, 5064−5073.
Robinson, A. L. (1932) *J. Am. Chem. Soc. 54*, 1311−1318.
Saran, A., Srivastava, S., Coutinho, E., & Maiti, M. (1995) *Indian J. Biochem. Biophys. 32*, 74−77.
Snyder, J. G., Hartman, N. G., D'Estantoit, B. L., Kennard, O., Remeta, D. P., & Breslauer, K. J. (1989) *Proc. Natl. Acad. Sci. U.S.A. 86*, 3968−3972.
Sobell, H. M., & Jain, S. C. (1972) *J. Mol. Biol. 68*, 21−34.
Spink, N., Brown, D. G., Skelly, J. V., & Neidle, S. (1994) *Nucleic Acids Res. 22*, 1607−1612.
Srinivasan, A. R., & Olson, W. K. (1987) *J. Biomol. Struct. Dyn. 4*, 895−938.
Sun, Q., Gatto, B., Yu, C., Liu, A., Liu, L. F., & LaVoie, E. J. (1994) *Bioorg. Med. Chem. Lett. 4*, 2871−2876.
Sun, Q., Gatto, B., Yu, C., Liu, A., Liu, L. F., & LaVoie, E. J. (1995) *J. Med. Chem. 38*, 3638−3644.
Takusagawa, F., Dabrow, M., Neidle, S., & Berman, H. M. (1982) *Nature 296*, 466−469.
Trask, D. K., & Muller, M. T. (1988) *Proc. Natl. Acad. Sci. U.S.A. 85*, 1417−1421.
Wang, L.-K., Johnson, R. K., & Hecht, S. M. (1993) *Chem. Res. Toxicol. 6*, 813−818.
Wassermann, K., Markovits, J., Jaxel, C., Capranico, G., Kohn, K. W., & Pommier, Y. (1990) *Mol. Pharmacol. 38*, 38−45.
Wilson, R. W., & Schellman, J. A. (1978) *Biopolymers 17*, 1235−1248.
Wilson, W. D., Gough, A. N., Doyle, J. J., & Davidson, M. W. (1976) *J. Med. Chem. 19*, 1261−1263.
Yamashita, Y., Kawada, S., Fujii, N., & Nakano, H. (1991) *Biochemistry 30*, 5838−5845.
Yamashita, Y., Fujii, N., Murakata, C., Ashizawa, T., Okabe, M., & Nakano, H. (1992) *Biochemistry 31*, 12069−12075.
Yoshinari, T., Yamada, A., Uemura, D., Nomura, K., Arakawa, H., Kojiri, K., Yoshida, E., Suda, H., & Okura, A. (1993) *Cancer Res. 53*, 490−494.
Zee-Cheng, K. Y., & Cheng, C. C. (1973) *J. Pharm. Sci. 62*, 1572−1573.
Zhurkin, V. B., Poltev, V. I., & Florent'ev, V. L. (1980) *Mol. Biol. (Moscow) 14*, 1116−1130.

BI971272Q